ISSN: 2277-5536 (Print); 2277-5641 (Online)

STRUCTURAL, MORPHOLOGICAL AND DIELECTRIC PROPERTIES OF NICKEL ZINC FERRITE NANOPARTICLES

Shahane G. S. * and Zipare K. V. **

*Department of Electronics, DBF Dayanand College of Arts and Science, Solapur, Maharashtra, India

**Department of Physics, CBK's Arts, Science and Commerce College Akkalkot, Maharashtra, India

(*E-mail: shahanegs@yahoo.com)

ABSTRACT

Nickel substituted zinc ferrite nanoparticles of the composition $Ni_xZn_{1-x}Fe_2O_4$ (x=0.1, 0.3, 0.5) have been synthesized by the chemical co-precipitation method. The samples were characterized by X-ray diffraction, transmission electron microscopy (TEM), and dielectric studies. The X-ray diffraction patterns confirm the synthesis of single crystalline phase of $Ni_xZn_{1-x}Fe_2O_4$ nanoparticles. Lattice parameter decreases with the increase in nickel content. On annealing the samples at 300°C an improvement in the crystal structure is observed. TEM studies reveal that the sample contains well dispersed nanoparticles with average particle size is of the order of 20 nm. The dielectric constant decreases with increase in frequency, showing dispersion in low frequency range and follows the Maxwell–Wagner interfacial polarization.

KEY WORDS: Dielectric properties, Ni-Zn ferrite nanoparticles, structural characterization,

INTRODUCTION

Nanocrystalline Ni-Zn ferrites are of great importance due to their wide range of potential applications such as transformer cores, high-density information storage devices, radar-absorbing materials, magnetic fluids, etc. (Costa *et al*. 2003; Virden *et al*. 2005; Lima *et al*. 2008). At the nano scale, the reduction in size leads to interesting magnetic properties, such as spin canting, surface effects, enhanced anisotropy and superparamagnetism (Caruntu *et al*., 2007). Nickel-Zinc ferrites are known to exist as mixed spinel structure. The compositional variation in these ferrites results in the redistribution of metal ions over the tetrahedral and octahedral sites which can modify the properties of ferrites. Among the various processes, chemical co-precipitation is the most convenient method for the synthesis of nanomagnetic particles as it is very simple and has better control over crystallite size and other properties of the materials (Sahoo *et al.* 2005; Gul *et al.* 2008; Rao *et al.* 2010). This paper reports the results of structural, morphological and dielectric properties of nickel substituted zinc ferrite nanoparticles with various compositions, synthesized by chemical co-precipitation method.

MATERIALS AND METHODS

Nanocrystalline $Ni_xZn_{1-x}Fe_2O_4$ particles with compositions (x=0.1, 0.3, 0.5) have been synthesized by a chemical co-precipitation method (Shahane *et al.* 2010). The starting materials used were AR grade $NiCl_2\,6H_2O$, $ZnCl_2$ and $FeCl_3$. For synthesis, equimolar solutions of $NiCl_2\,6H_2O$, $ZnCl_2$ and $FeCl_3$ were mixed in their stoichiometric ratio and homogenized at 60°C. The pH of the solution was maintained at 8.5 by adding ammonia solution with constant stirring. The mixture was then heated at 80°C for about one hour. The precipitated particles were then washed several times with double distilled water to remove the salt residues and other impurities. It was further dried at 80°C to obtain the powder. The samples were annealed at 300°C in the argon atmosphere for one hour. These samples were then characterized through various characterization techniques. The X-ray diffraction patterns were recorded using a Rigaku powder X-ray diffractometer with Cu K_α(λ=1.54059Å) radiation. The TEM was recorded on transmission electron microscope (Model - JEOL JEM – 200 CXV). The dielectric studies of the samples were carried out in the frequency range 100 Hz to 1 MHz using experimental set up Wayne-Kerr (model 6540 A). The Dielectric constant is measured using the relation, $\varepsilon' = Cd/\varepsilon_0 A$, where C is the capacitance of the sample, d is the thickness; A is the area of the flat surface of the pellet and ε_0 the constant of permittivity of the free space.

RESULTS AND DISCUSSION

Figure 1(A, B) shows the powder X-ray diffraction patterns for as-synthesized and annealed samples with various nickel and zinc compositions. The 'd' values and intensities of observed diffraction peaks match with the single crystalline spinel form of the nickel zinc ferrite (JCPDS Card No. 019-0629). X-ray diffraction pattern shows broad peaks indicating small crystallite size of the particles. On annealing the samples at 300°C the X-ray diffraction patterns show an improvement in the sharpness and intensity of the peaks. The lattice parameters were calculated for all the compositions and are listed in Table 1. It is observed that lattice parameter decreases with increase in nickel content. The higher value of lattice parameter in $Ni_{0.1}Zn_{0.9}Fe_2O_4$ sample can be attributed to larger radius of Zn^{2+} cation. The decrease in lattice parameter with increase in nickel content is due to the replacement of larger Zn^{2+} cation by smaller Ni^{2+}cation (Popovici *et al.* 2003; Gul *et al.* 2008). The induced strain in the crystallites has been calculated (Table 1). It is found that strain is maximum for zinc rich sample and decreases as nickel concentration increases. The crystallite size was then determined by the Scherrer's relation and the values are listed in Table 1. On annealing the crystallite size

increases gradually and is attributed to the grain growth of the particles in the nano region at the temperatures well below the melting temperature of the bulk ferrites.

Table1: X-ray analysis of as-synthesized and annealed (300°C) $Ni_xZn_{1-x}Fe_2O_4$ samples.

Comp. x	Lattice parameter (Å)		Strain		Crystallite Size (nm)	
	(raw)	(300°C)	(raw)	(300°C)	(raw)	(300°C)
0.1	8.4271	8.4244	0.003539	0.003428	11.85	13.71
0.3	8.4100	8.4160	0.002446	0.002241	13.34	16.61
0.5	8.4093	8.4091	0.002166	0.001859	16.76	18.37

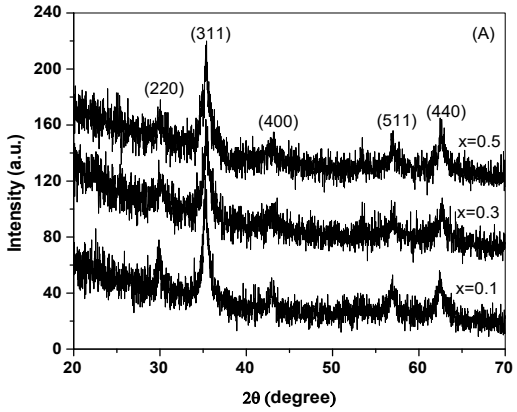

Figure 1(A): X-ray diffractograms of as-synthesized $Ni_xZn_{1-x}Fe_2O_4$ samples.

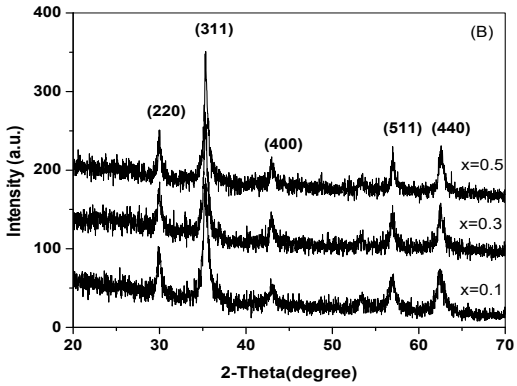

Figure 1(B): X-ray diffractograms of $Ni_xZn_{1-x}Fe_2O_4$ samples annealed at 300°C.

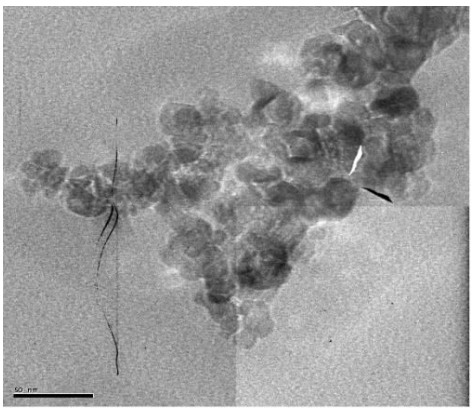

Figure 2: TEM image of $Ni_{0.3}Zn_{0.7}Fe_2O_4$ sample.

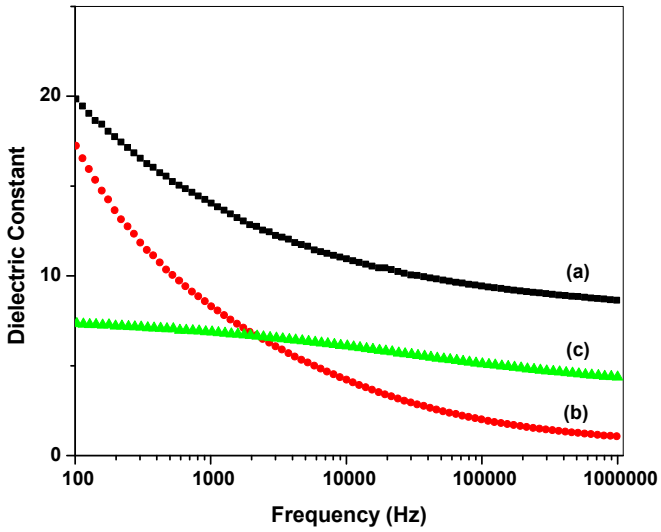

Figure 3: Frequency dependence of dielectric constant for $Ni_{1-x}Zn_xFe_2O_4$ ferrite nanoparticles (a) x=0.1, (b) x=0.3 and (c) x=0.5.

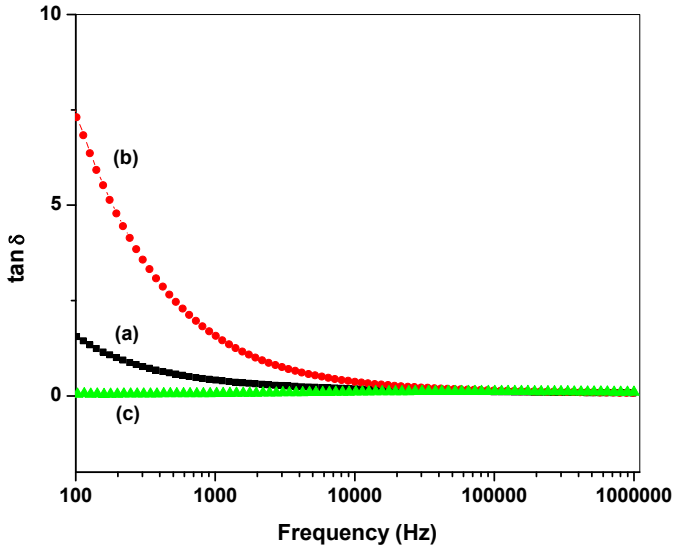

Figure 4: Variation of dielectric loss tangent for various $Ni_{1-x}Zn_xFe_2O_4$ nanoparticles (a) x=0.1, (b) x=0.3 and (c) x=0.5.

The transmission electron microscopy was used to study the morphology and structure of the samples. Figure 2 shows the TEM image of as-prepared Ni-Zn sample with x=0.3. The sample contains well dispersed nanoparticles with average particle size is of the order of 20 nm. The particle size determined from TEM was found to be in good agreement with that obtained from XRD studies.

The frequency dependence of the dielectric constant for all the samples was studied at room temperature. The variation in dielectric constant (ε') with frequency at room temperature for the various $Ni_xZn_{1-x}Fe_2O_4$ samples is shown in Figure 3. It is seen that the dielectric constant decreases with increase in frequency, showing dispersion in low frequency

range. The decrease in ε' is rapid at lower frequencies and showed almost frequency-independent behavior at higher frequencies indicating Maxwell–Wagner type of interfacial polarization (Gull *et al.* 2008; Nasir *et al.* 2011; Hashim *et al.* 2012). The decrease in dielectric constant with frequency can be explained on the basis that the solid is assumed as composed of well conducting grains and is separated by non-conducting grain boundaries, when electrons reach such non conducting grain boundaries through hopping the resistance of the grain boundary is high, hence the electron pile up at the grain boundaries and produce polarization. As frequency increases, electrons do not follow the alternating field. This decreases the probability of electrons reaching the grain boundary and as a result polarization decreases (Ravinder *et al.* 2001; Gangatharan *et al.* 2010; Nasir *et al.* 2011). Figure 4 shows the variation of dielectric loss tangent with frequency at room temperature. It is seen that dielectric loss tangent decrease with increase in frequency which is a normal behavior of any ferrite material. The dielectric loss decreases rapidly in the low-frequency region, while the rate of decrease is slow in the high-frequency region, and it shows an almost frequency independent behavior in the high-frequency region. The low loss values at higher frequencies show the potential applications of these materials in high-frequency microwave devices (Batoo *et al.* 2012).

CONCLUSION

A low temperature chemical co-precipitation method is successfully used for synthesis of nanocrystalline nickel zinc ferrite particles with various compositions. The X-ray diffraction patterns confirm the synthesis of single crystalline phase of $Ni_xZn_{1-x}Fe_2O_4$ (x=0.1, 0.3, 0.5) nanoparticles. Lattice parameter decreases with the increase in nickel content. TEM studies support the nanocrystalline nature of the samples as observed from XRD studies. The dielectric constant follows the Maxwell–Wagner interfacial polarization.

REFERENCES

Batoo K.M. and Ansari M.S. (2012). Low temperature-fired Ni-Cu-Zn ferrite nanoparticles through auto-combustion methodfor multilayer chip inductor applications. *Nanoscale Res. Lett.* **7:** 112-125.

Caruntu D., Caruntu G. and O'Connor C. J. (2007). Magnetic properties of variable sized Fe_3O_4 nanoparticles synthesized from non-aqueous homogeneous solutions of polyols. *J. Phys. D: Appl. Phys.***40:** 5801-5809.

Costa A. C. F. M., Tortella E., Morelli M. R. and Kiminami R. H. G. A. (2003). Synthesis, microstructure and magnetic properties of Ni-Zn ferrites. *J. Magn. Magn. Mater.* **256:** 174-182.

Gangatharan S., Chidambaram V. and Kandasamy S. (2010). Synthesis, Structural and Dielectric Studies of Nickel Substituted Cobalt-Zinc Ferrite. *Mater. Sci. Appl.***1:** 19-24.

Gul I.H., Ahmed W., Maqsood A. (2008). Electrical and magnetic characterization of nanocrystalline Ni–Zn ferrite synthesis by co-precipitation route. *J. Magn. Magn. Mater.* **320:**270-275.

Hashim M, Alimuddin, Shalendra Kumar, Sikander A., Koo B.H., Chung H. and Ravi Kumar (2012). Structural, magnetic and electrical properties of Al^{3+} substituted Ni- Zn ferrite nanoparticles. *J. Alloys Compounds*. **511(1):**107-114.

Lima U.R., Nasar M.C., Nasar R.S., Rezende M.C. and Araujoc J. H. (2008). Ni–Zn nanoferrite for radar-absorbing material. *J. Magn. Magn. Mater.* **320:** 1666-1670.

Nasir S., Anis-ur-Rehman M. and Malik M. A. (2011). Structural and dielectric properties of Cr-doped Ni–Zn nanoferrites. *Phys. Scr.* **83:**025602-5.

Popovici M., Savii C., Niznansky D., Subrt J., Bohacek J., Becherescu D., Caizer C., Enache C. and Ionescu C. (2003). Nanocrystalline Ni-Zn ferrites prepared by sol-gel method. J. Optoelect. & Adv. Mater.**5 (1):** 25-256.

Rao P.B.C, and Setty S.P. (2010). Electrical properties of Ni-Zn nano ferrite particles. *Inter. J. Engin. Sci. and Tech.* **2(8):** 3351-3354.

Ravinder D. and Vijaya Kumar K. (2001). Dielectric behaviour of erbium substituted Mn–Zn ferrites. *Bull. Mater. Sci.* **24 (5):** 505-509.

Sahoo Y., Goodarzi A., Swihart M. T., Ohulchansky T. Y., Kaur N., Fulani E. P. and Prasad P. N.(2005). Aqueous Ferrofluid of Magnetic Nanoparticles: Fluorescence Labeling and Magnetophoretic Control. *J. Phys. Chem. B.***109:** 3879-3885.

Shahane G.S., Ashok Kumar, Arora M., Pant R.P. and Krishan Lal (2010). Synthesis and characterization of Ni–Zn ferrite nanoparticles. *J. Magn. Magn. Mater.* **322:**1015-1019.

Virden A. E. and O'Grady K. (2005). Structure and magnetic properties of NiZn ferrite nanoparticles. *J. Magn. Magn. Mater*. **290:** 868-870.